

AFRL-PR-WP-TP-2006-265

**HYDROXYL TAGGING
VELOCIMETRY IN A MACH 2 FLOW
WITH A WALL CAVITY
(POSTPRINT)**



**R.W. Pitz, M.D. Lahr, Z.W. Douglas, J.A. Wehrmeyer, S. Hu,
C.D. Carter, K.-Y. Hsu, C. Lum, and M.M. Koochesfahani**

OCTOBER 2006

Approved for public release; distribution is unlimited.

STINFO COPY

© 2005 Robert W. Pitz

**The U.S. Government is joint author of the work and has the right to use, modify,
reproduce, release, perform, display, or disclose the work.**

**PROPULSION DIRECTORATE
AIR FORCE MATERIEL COMMAND
AIR FORCE RESEARCH LABORATORY
WRIGHT-PATTERSON AIR FORCE BASE, OH 45433-7251**

REPORT DOCUMENTATION PAGE

Form Approved
OMB No. 0704-0188

The public reporting burden for this collection of information is estimated to average 1 hour per response, including the time for reviewing instructions, searching existing data sources, gathering and maintaining the data needed, and completing and reviewing the collection of information. Send comments regarding this burden estimate or any other aspect of this collection of information, including suggestions for reducing this burden, to Department of Defense, Washington Headquarters Services, Directorate for Information Operations and Reports (0704-0188), 1215 Jefferson Davis Highway, Suite 1204, Arlington, VA 22202-4302. Respondents should be aware that notwithstanding any other provision of law, no person shall be subject to any penalty for failing to comply with a collection of information if it does not display a currently valid OMB control number. **PLEASE DO NOT RETURN YOUR FORM TO THE ABOVE ADDRESS.**

1. REPORT DATE (DD-MM-YY) October 2006		2. REPORT TYPE Conference Paper Postprint		3. DATES COVERED (From - To) N/A				
4. TITLE AND SUBTITLE HYDROXYL TAGGING VELOCIMETRY IN A MACH 2 FLOW WITH A WALL CAVITY (POSTPRINT)				5a. CONTRACT NUMBER In-house				
				5b. GRANT NUMBER				
				5c. PROGRAM ELEMENT NUMBER 61102F				
6. AUTHOR(S) R.W. Pitz, M.D. Lahr, Z.W. Douglas, J.A. Wehrmeyer, and S. Hu (Vanderbilt University) C.D. Carter (AFRL/PRAS) K.-Y. Hsu (Innovative Scientific Solutions, Inc.) C. Lum and M.M. Koochesfahani (Michigan State University)				5d. PROJECT NUMBER 2308				
				5e. TASK NUMBER AI				
				5f. WORK UNIT NUMBER 00				
7. PERFORMING ORGANIZATION NAME(S) AND ADDRESS(ES) <table style="width: 100%; border: none;"> <tr> <td style="width: 33%; border: none;">Vanderbilt University Department of Mechanical Engineering Nashville, TN 37235</td> <td style="width: 33%; border: none;">Propulsion Sciences Branch (AFRL/PRAS) Aerospace Propulsion Division Propulsion Directorate Air Force Research Laboratory Air Force Materiel Command Wright-Patterson AFB, OH 45433-7251</td> <td style="width: 33%; border: none;">Innovative Scientific Solutions, Inc. Dayton, OH 45440 ----- Michigan State University Department of Mechanical Engineering East Lansing, MI 48824</td> </tr> </table>				Vanderbilt University Department of Mechanical Engineering Nashville, TN 37235	Propulsion Sciences Branch (AFRL/PRAS) Aerospace Propulsion Division Propulsion Directorate Air Force Research Laboratory Air Force Materiel Command Wright-Patterson AFB, OH 45433-7251	Innovative Scientific Solutions, Inc. Dayton, OH 45440 ----- Michigan State University Department of Mechanical Engineering East Lansing, MI 48824	8. PERFORMING ORGANIZATION REPORT NUMBER AFRL-PR-WP-TP-2006-265	
				Vanderbilt University Department of Mechanical Engineering Nashville, TN 37235	Propulsion Sciences Branch (AFRL/PRAS) Aerospace Propulsion Division Propulsion Directorate Air Force Research Laboratory Air Force Materiel Command Wright-Patterson AFB, OH 45433-7251	Innovative Scientific Solutions, Inc. Dayton, OH 45440 ----- Michigan State University Department of Mechanical Engineering East Lansing, MI 48824		
9. SPONSORING/MONITORING AGENCY NAME(S) AND ADDRESS(ES) Propulsion Directorate Air Force Research Laboratory Air Force Materiel Command Wright-Patterson AFB, OH 45433-7251				10. SPONSORING/MONITORING AGENCY ACRONYM(S) AFRL-PR-WP				
				11. SPONSORING/MONITORING AGENCY REPORT NUMBER(S) AFRL-PR-WP-TP-2006-265				
12. DISTRIBUTION/AVAILABILITY STATEMENT Approved for public release; distribution is unlimited.								
13. SUPPLEMENTARY NOTES Conference paper published in the Proceedings of the 2005 43rd AIAA Aerospace Sciences Meeting and Exhibit, published by AIAA. © 2005 Robert W. Pitz. The U.S. Government is joint author of the work and has the right to use, modify, reproduce, release, perform, display, or disclose the work. PAO case number: AFRL/WS 04-1495; Date cleared: 28 Dec 2004. Paper contains color.								
14. ABSTRACT Hydroxyl tagging velocimetry (HTV) measurements of velocity were made in a Mach 2 flow with a wall cavity. In the HTV method, ArF excimer laser (193 nm) beams pass through a humid gas and dissociate H ₂ O into H + OH to form a tagging grid of OH molecules. In this study, a 7x7 grid of hydroxyl (OH) molecules is tracked by planar laser-induced fluorescence. The grid motion over a fixed time delay yields about 50 velocity vectors of the two-dimensional flow. Instantaneous, single-shot measurements of two-dimensional flow patterns were made in the non-reacting Mach 2 flow with a wall cavity under low and high pressure conditions. The single-shot profiles were analyzed to yield mean and rms velocity profiles in the Mach 2 non-reacting flow.								
15. SUBJECT TERMS								
16. SECURITY CLASSIFICATION OF:			17. LIMITATION OF ABSTRACT: SAR	18. NUMBER OF PAGES 20	19a. NAME OF RESPONSIBLE PERSON (Monitor) Campbell D. Carter 19b. TELEPHONE NUMBER (Include Area Code) N/A			
a. REPORT Unclassified	b. ABSTRACT Unclassified	c. THIS PAGE Unclassified						

Hydroxyl Tagging Velocimetry in a Mach 2 Flow with a Wall Cavity

R. W. Pitz^{*}, M. D. Lahr[†], Z. W. Douglas[‡], J. A. Wehrmeyer[§], and S. Hu^{**}
Department of Mechanical Engineering, Vanderbilt University, Nashville, Tennessee 37235

C. D. Carter^{††}
Air Force Research Laboratory (AFRL/PRAS), Wright-Patterson Air Force Base, Ohio 45433

K.-Y. Hsu^{‡‡}
Innovative Scientific Solutions, Inc., Dayton, Ohio 45440

and

C. Lum^{§§} and M. M. Koochesfahani^{***}
Department of Mechanical Engineering, Michigan State University, East Lansing, MI 48824

Hydroxyl tagging velocimetry (HTV) measurements of velocity were made in a Mach 2 flow with a wall cavity. In the HTV method, ArF excimer laser (193 nm) beams pass through a humid gas and dissociate H₂O into H + OH to form a tagging grid of OH molecules. In this study, a 7x7 grid of hydroxyl (OH) molecules is tracked by planar laser-induced fluorescence. The grid motion over a fixed time delay yields about 50 velocity vectors of the two-dimensional flow. Instantaneous, single-shot measurements of two-dimensional flow patterns were made in the non-reacting Mach 2 flow with a wall cavity under low and high pressure conditions. The single-shot profiles were analyzed to yield mean and rms velocity profiles in the Mach 2 non-reacting flow.

I. Introduction

Non-intrusive measurements of velocity are needed in supersonic flow where probes easily produce flow disturbances. Non-intrusive gas phase velocity measurements are normally made with laser scattering from particles that naturally exist in the flow or are added to the flow. Particle-based velocity methods include techniques such as laser-Doppler velocimetry (LDV), particle image velocimetry (PIV), planar Doppler velocimetry (PDA), and phase

^{*} Prof. and Department Chair, Department of Mechanical Engineering, VU Station B 351592, 2301 Vanderbilt Place, Nashville, TN 37235-1592, AIAA Associate Fellow

[†] Graduate Student, Mechanical Engineering Department, VU Station B 351592, 2301 Vanderbilt Place, Nashville, TN 37235-1592, AIAA Student Member

[‡] Undergraduate Student, Mechanical Engineering Department, VU Station B 351592, 2301 Vanderbilt Place, Nashville, TN 37235-1592, Non-member

[§] Adjoint Associate Prof., 1099 Avenue C, Arnold AFB, TN 37389-9013, AIAA Senior Member

^{**} Graduate Student, Mechanical Engineering Department, VU Station B 351592, 2301 Vanderbilt Place, Nashville, TN 37235-1592, AIAA Student Member

^{††} Senior Aerospace Engineer, Aerospace Propulsion Division (AFRL/PRA), 1950 Fifth St., Wright-Patterson Air Force Base, OH 45433, AIAA Associate Fellow

^{‡‡} Research Scientist, Innovative Scientific Solutions, Inc., 2766 Indian Ripple Rd., Dayton, OH 45440, AIAA Associate Fellow

^{§§} Graduate Student, Department of Mechanical Engineering, Michigan State University, East Lansing, MI 48824, Non-member

^{***} Professor, Department of Mechanical Engineering, Michigan State University, East Lansing, MI 48824, AIAA Associate Fellow

Doppler velocimetry (PDV).^{1,2} In supersonic flow, the particle velocity often differs from the actual gas velocity due to particle drag and slow response to velocity gradients.³ Also in confined flows, the particles can coat the windows leading to limited test times or even window abrasion.⁴

Laser-based molecular velocity methods directly measure the gas velocity. In Doppler shift methods, the small Doppler shift of the wavelength of the scattered laser light is measured and related to the velocity. These methods are more accurate at higher velocities as the Doppler shift is larger and more easily measurable; but they often only yield average flow velocities due to a lack of signal strength. Many of these Doppler-based molecular velocity methods are based on laser-induced fluorescence of molecules (or atoms) that are added to the flows such as copper⁵, hydroxyl^{6,7}, nitric oxide⁸, sodium⁹ and iodine¹⁰. The addition of such molecules is often not practical in test facilities. Also in Doppler shift methods, the optical geometry of the laser and observer define the velocity component that is measured, and this feature can be limiting.¹¹ Other Doppler shift velocity methods are based on Rayleigh scattering from the gas molecules¹²⁻¹³ but Rayleigh scattering signals are low and are difficult to obtain in confined facilities due to interference from laser scattering from the walls and particles in the flow.¹¹

Molecular tagging methods measure the gas velocity by time-of-flight. The molecules in the gas flow are tagged or marked with a laser, and the movement of the tag gives the velocity. Once a laser line or grid is tagged, the grid will move with the flow. The movement of the tagged regions is imaged by a method dictated by the photochemistry of the tagged molecules (laser-induced fluorescence in the case of HTV). The displacement of tagged grid over a fixed time period yields the velocity.

Many molecular tagging methods use a gas “seed”. A gas molecule (or atom) is added to the flow and the molecule is tagged with a laser beam (e.g., electronically excited, photo-dissociated, or vibrationally excited). In gas seeded methods, the flow is seeded with molecules (or atoms) such as acetone¹⁴, biacetyl^{15,16}, nitric oxide^{11,17}, nitrogen dioxide¹⁸, sodium¹⁹, strontium²⁰ or tert-butyl nitrate.²¹ For test facility flows, the addition of these atomic/molecular seeds is often undesirable due to a variety of factors (e.g., seed toxicity, expense, etc.).

There are “unseeded” tagging methods where gas tags are produced from molecules naturally occurring in air (i.e., nitrogen, oxygen, water vapor). Examples of molecular tags produced from air are N_2^+ ion²², ozone²³⁻²⁵, hydroxyl²⁵⁻³⁰, nitric oxide³¹⁻³³, and vibrationally excited oxygen^{34,35}. Many of the methods use non-linear laser excitation^{22,26,31-35} to produce these tags from air and the tag is only produced in a small region near the laser focus. In this work, hydroxyl tagging velocimetry is used which is a linear method²⁸⁻³⁰. An ArF laser at 193nm photodissociates water in a single photon process to produce OH in a grid. The OH grid moves for a known period of time and the position of the grid is recorded with laser-induced fluorescence of OH.

Accurate non-intrusive velocity data are limited in high speed, compressible flows, in part due to biasing effects when applying conventional particle-based laser velocity methods.³ Non-intrusive velocity data are needed in flows relevant to scramjet combustion and molecular-based methods such as hydroxyl tagging velocimetry avoid the problems associated with particle based methods. In scramjets, wall cavities are commonly used to stabilize combustion with minimal pressure drag.³⁶ An optically accessible supersonic flow facility has been developed to study cavity flows to understand supersonic reacting flow and to compare the results to advanced CFD models.³⁷⁻³⁹ In this work, the HTV method is applied to a Mach 2 flow with a wall cavity to obtain instantaneous two-dimensional velocity images, mean velocity profiles and rms velocity profiles. Velocity measurements are made using HTV in the free-stream and the cavity of the Mach 2 cavity-piloted combustor.

II. Experimental System

The experiments were conducted at the supersonic flow facility in Research Cell 19 at the Air Force Research Laboratory, Propulsion Directorate at Wright-Patterson Air Force Base. The tunnel has a two-dimensional Mach 2 nozzle. The air flow rate is about 1.5 kg/sec. A schematic of the test configuration is shown in Figure 1. Fused silica windows (Suprasil, with good transmission at 193 nm) form the side walls of the tunnel. The tunnel has a constant-area “isolator” section upstream of the cavity with a cross-section of 51 mm high by 153 mm wide; downstream of the isolator, the bottom wall diverges at an angle of 2.5°. A cavity to provide a flame pilot is in the bottom of the tunnel as shown in Fig. 1. The cavity is 17 mm deep and 66 mm long. A shear layer forms at the edge of the first step in the cavity and the recirculation zone is produced by the cavity.

A schematic of the HTV system is shown in Fig. 2. The ArF excimer laser beam (20 mm high by 10 mm wide, 115 mJ/pulse, broadband, 1 nm bandwidth) is split into two beams by a beam splitter. Each of the laser beams is sent through grid forming optics that produces two sets of 7 beams each. The grid optics consist of two major components placed very close together: a 300 mm focal length cylindrical lens (25 mm x 40 mm) and a stack of 300 mm cylindrical lenses (20 mm wide by 3 mm high). The beam diameter is about 0.3 mm diameter in the measurement zone. The sets of beams produce 49 crossing points in the measurement zone.

The 7 x 7 grid of ArF-generated “lines” of OH was imaged by laser-induced fluorescence of OH using the $Q_1(1)$ transition of the $A^2\Sigma^+ (v' = 1) \leftarrow X^2\Pi_i (v'' = 0)$ band at 282 nm. A Spectra Physics Model GRC 170 Nd:YAG laser pumped a Lumonics HD-300 Hyperdye dye laser. The output of the dye laser was doubled by an Inrad Autotracker II to produce about 20 mJ/pulse of 282 nm laser radiation. A small portion of the 282 nm beam was split off and directed over a small flame and then to a photodiode. Signals from the photodiode and a photomultiplier tube—recording the OH laser-induced fluorescence from the flame—were displayed on an oscilloscope to ensure proper operation of the dye laser and good overlap with the OH transition. Timing of the lasers and camera was accomplished with a Quantum Composer (model 9318E) pulse generator. Random (shot-to-shot) timing error between the lasers was about ± 20 ns or about $\pm 1\%$ of the typical 2 μ s timing separation.

The OH-probe laser beam was expanded by a negative cylindrical lens (focal length = -150 mm) and focused by a 1000 mm focal length spherical lens to form a sheet. To improve the signal strength, the laser sheet was retro-reflected through the tunnel, with a delay of about 5 ns. Both this sheet and the 193 nm grid were rotated to be parallel to the tunnel bottom floor (2.5° off the horizontal plane).

Fluorescence from the created OH was recorded using a PIMAX “Superblue” intensified CCD camera, which was fitted with a 45-mm f/1.8 UV lens (Cerco). Schott glass filters (WG-295 or 305 and UG-11) were employed to block background scattering and fluorescence (from tunnel surfaces). Typically, the 512 x 512 pixel array of the PIMAX camera was binned 2 x 2 to improve the signal strength. The field of view was 40 mm square, and the camera looked down on the cavity through the tunnel top window. Each 2x2 binned pixel is 156 μ m x 156 μ m. The region probed was roughly in the spanwise center of the flowfield.

Focusing optics (for both laser systems) and the CCD camera were mounted on a three-dimensional traversing table located beneath the tunnel; the lasers, however, were not mounted on this table. The optics between the lasers and traversing table were thus arranged to allow the laser grid/sheet height location to be varied and thus the shear layer and cavity to be probed.

With stagnant room air in the tunnel at 1 atm. pressure, the ArF laser was pulsed to create the OH grid that was subsequently excited by the OH-probe laser sheet after a short delay (~ 0.2 μ sec). The fluorescence signal was recorded by the ICCD camera and the OH probe laser wavelength was scanned over about 0.7 nm. The resultant laser excitation scan is shown in Fig. 3. The measured spectrum was compared to a simulated spectrum calculated by LIFbase (ver. 2).⁴⁰ The measured and calculated line positions match very well. At room temperature (295K), the strongest line is the combined $Q_1(1) + R_2(3)$ peak in the OH A-X (1,0) band. Thus the OH probe laser was tuned to this line for the maximum signal.

III. Results

HTV measurements were made in air with no fuel addition. The conditions for the non-reacting flow are given in Table 1. Test A is the “low backpressure” condition where the backpressure valve downstream of the test section is fully open. Test B is the “high backpressure condition where the backpressure valve is 64% closed. The “high backpressure” condition simulates the pressure rise from main-duct combustion. Under “low backpressure” conditions the tunnel flow above the cavity is largely free of shock waves (see Fig. 2 in reference 39). Under “high backpressure” conditions, shocks are seen above the cavity.³⁹

Since the tunnel air was dried, water was sprayed into the stagnation chamber to provide moist air. No water droplets were observed in the test section. HTV measurements were made in the spanwise direction in the tunnel. The position of the measured OH grids in regards to the cavity walls is shown in Fig. 4. Examples of two-dimensional instantaneous velocity images from the HTV method are shown in Figs. 5, 6, and 7. Fig. 5 is an example of an undisplaced averaged HTV image used as the reference for the displaced grid patterns. The velocity vectors in Figs. 6 and 7 are shown on top of the displaced HTV grid pattern. The displacement of each grid intersection is determined by a direct digital spatial correlation techniques using an in-house code.⁴¹ A small region surrounding a grid intersection in the undisplaced image, referred to as the source window, is spatially correlated with a larger roam window in the delayed image. The location of the peak of the correlation coefficient is identified as the displacement vector, which after division by the time delay between the two images provides the estimate of the spatial average of the velocity within the source window. Sub-pixel accuracy is achieved using a multi-dimensional polynomial fit to the region near the correlation peak. The details of this procedure and its performance are described by Gendrich and Koochesfahani.⁴¹ In this work, the time delay is either 2 or 3 μ s.

The molecular tagging velocimetry data is obtained originally on an irregularly spaced measurement grid. To take advantage of standard data display and processing techniques, the MTV data is remapped onto a grid with uniform spacing. The remapping is done using a local least-squares fit to a two dimensional 2nd order polynomial.

The irregular grid and regular grid spacing applied to the HTV measurements is shown in Figs. 6 and 7. The irregular grid pattern shown on the left is fit with this procedure onto the regular grid shown on the right. The details of the procedure and its performance characteristics are given by Cohn and Koochesfahani⁴².

In the freestream above the cavity shown in Fig. 6, the velocity pattern is very uniform with a value of about 680 m/s (note reference vector of 1000 m/s). The higher velocity (than expected for the Mach 2 nozzle) arises from the divergence of the bottom wall. In the cavity the flow reverses, and the velocity pattern is much more variable as seen in Fig. 7. The velocities in the cavity are reversed with a negative velocity of about 60 m/s (note reference vector of 200 m/s).

The average signal-to-noise ratio of the single-shot images is about 7-13. With a crossing angle of about 150 degrees, the center of the line crossings can be determined to about 0.1 pixels or a displacement of 16 μm according to previous calculations (see Fig. 5 in reference 41). Thus the accuracy of the velocity measurement is about 8 m/s.

The instantaneous velocity images were analyzed to obtain mean and rms velocities. The streamwise mean velocity profiles for the low backpressure case are shown in Fig. 9. Each data point is an average of 100 instantaneous values obtained from the images. Streamwise profiles are shown near the centerline of the flow from the freestream to down in the cavity. The locations of the profiles shown in the plots is shown in Fig. 8. The velocities above the cavity are about 680 m/s and decrease in the shear layer and become negative (about -60 m/s) in the cavity. The shear layer profile appears typical of flows formed behind a rearward facing step.⁴³ The shear layer width grows with downstream distance.

The rms velocities for the low back pressure case are shown in Fig. 10. The rms values in the freestream are as low as 15 m/s or about 2.2%. This rms value is due to a combination of freestream turbulence and measurement precision. Recall that the timing error is about $\pm 1\%$ of the typical 2 μs delay and the distance error is about 16 μm , equaling 8 m/s or about 1.2%; of course, the timing error could largely be eliminated by recording with a photodiode the timing for each image. The rms values increase in the shear layer and decrease slightly in the cavity similar to what is observed in the flow behind a backward facing step.⁴³

The mean and rms values for the high back pressure case are shown in Figs. 11 and 12. The profiles are drastically changed from the low back pressure case. Shock waves observed previously³⁹ greatly modify the mean and rms values of the velocity. These profiles do not correspond to those seen in subsonic flows behind a backward facing step.⁴³ In this unsteady compressible flow with shocks, the mean velocity profile is almost linear above the cavity. The rms values are highest above the cavity where shocks have been previously observed (see Fig. 2 in reference 39).

IV. Conclusions

Non-intrusive measurements of velocity are obtained in a Mach 2 flow with a wall cavity using hydroxyl tagging velocimetry under low and high backpressure conditions. Instantaneous two-dimensional images are obtained in the freestream and the cavity. The instantaneous planar measurements are analyzed to determine the mean and rms velocities in the streamwise direction. Under high pressure conditions, the shocks in the cavity greatly modify the mean velocity profiles and greatly increase the rms velocity values. These measurements demonstrate the utility of the hydroxyl tagging method. Here, with only the addition of water to the flow, high fidelity measurements of the flowfield velocity of a high-speed flow above a recessed cavity are possible. Difficulties encountered with particle-based methods—especially in recirculation regions around high speed core flows—are obviated with this approach. Future work will explore in detail approaches to making measurements in reacting cavities (with high-speed cross flows) and the use of a greater number of grids (e.g., 10×10 and/or 12×12).

Acknowledgements

This research was supported by the Air Force Office of Scientific Research under the support of J. Tishkoff. RWP was supported by an AFOSR Summer Faculty Fellowship and Arnold Engineering Development Center under contract No. F40600-03-D-0001.

References

1. Adrian, R. J., "Particle imaging techniques for experimental fluid mechanics," *Annu. Rev. Fluid Mech.*, **23**, 261-304 (1991).
2. Drain, L. E., *The Laser Doppler Technique*, (Wiley, New York, 1980).

3. Maurice, M. S., "Laser velocimetry seed particles within compressible, vertical flows," *AIAA J.* **30**, 376-383 (1992).
4. Santoro, R. J., Pal, S., Woodward, R. D., Schaaf, L., "Rocket testing at university facilities," *39th AIAA Aerospace Sciences Meeting and Exhibit*, Paper No. 0748 (2001).
5. Marinelli, W.J., Kessler, W.J., Allen, M.G., Davis, S.J., and Arepalli, S. (1991) "Copper atom based measurements of velocity in turbulence and in arc jet flows," *AIAA Paper 91-0358*, *29th AIAA Aerospace Sciences Meeting and Exhibit*, Reno, NV.
6. Allen, M., Davis, S., Kessler, W., Legner, H., McManus, K., Mulhall, P., Parker, T., and Sonnenfroh, D. "Velocity field imaging in supersonic reacting flows near atmospheric pressure," *AIAA J* **32**, 1676-1682 (1994)
7. Klavuhn, K. G., Gauba, G., McDaniel, J.C. OH laser-induced fluorescence velocimetry technique for steady, high-speed, reacting flows. *J. Propul. Power* **10**, 787-797 (1994).
8. Paul, P.H., Lee, M.P., Hanson, R.K., "Molecular velocity imaging of supersonic flows using pulsed planar laser-induced fluorescence of NO," *Opt. Lett.* **14**, 417-419 (1989).
9. Zimmermann, M. and Miles, R.B., "Hypersonic-helium-flow-field measurements with the resonant Doppler velocimeter," *Appl. Phys. Lett.* **37**, 885-887 (1980).
10. McDaniel, J.C., Hiller, B., and Hanson, R.K., "Simultaneous multiple-point velocity measurements using laser-induced iodine fluorescence," *Opt. Lett.* **8**, 51-53 (1983).
11. Houwing, A. F. P., Smith, D. R., Fox, J. S., Danehy, P. M. and Mudford, N. R., "Laminar boundary layer separation at a fin-body junction in a hypersonic flow," *Shock Waves* **11**, 31-42 (2001).
12. Seasholtz, R. G., Zupanc, F.J., Schneider, S. J., "Spectrally resolved Rayleigh scattering diagnostic for hydrogen-oxygen rocket plume studies," *J. Propul. Power* **8**, 935-942 (1992).
13. Miles, R.B., Lempert, W.R., "Quantitative flow visualization in unseeded flows," *Annu. Rev. Fluid Mech.* **29**, 285-326 (1997).
14. Lempert, W. R., Jiang, N., Sethuram, S., and Samimy, M., "Molecular tagging velocimetry measurements in supersonic microjets," *AIAA J.* **40**, 1065-1070 (2002).
15. Hiller, B., Booman, R. A., Hassa, C., and Hanson, R. K., "Velocity visualization in gas flows using laser-induced-fluorescence of biacetyl," *Rev. Sci. Instrum.* **55**, 1964-1967 (1984).
16. Stier, B. and Koochesfahani, N. M., "Molecular tagging velocimetry (MTV) measurements in gas phase flows," *Exp. Fluids* **26**, 297-304 (1999).
17. Danehy, P. M., O'Byrne, S., Houwing, A. F. P., Fox, J. S., and Smith, D. R., "Flow-tagging velocimetry for hypersonic flows using fluorescence of nitric oxide," *AIAA J.* **41**, 263-271 (2002).
18. Orlemann, C., Schulz, C., and Wolfrum, J., "NO-flow tagging by photodissociation of NO₂. A new approach for measuring small-scale flow structures," *Chem. Phys. Lett.* **307**, 15-20 (1999).
19. Barker, P., Thomas, A., Rubinsztein-Dunlop, H., Ljungberg, P., "Velocity measurements by flow tagging employing laser enhanced ionisation and laser induced fluorescence," *Spectrochim. Acta B* **50**, 1301-1310 (1995).
20. Rubinsztein-Dunlop H., Littleton, B., Barker, P., Ljungberg, P., and Malmsten, Y., "Ionic Strontium fluorescence as a method of flow-tagging velocimetry," *Exp. Fluids* **30**, 36-42 (2001).
21. Krüger, S. and Grünfeld, G., "Stereoscopic flow-tagging velocimetry," *Appl. Phys. B* **69**, 509-512 (1999)
22. Ress, J. M., Laufer, G., and Krauss, R. H., "Laser ion time-of-flight velocity measurements using N₂⁺ tracers," *AIAA J.* **33**, 296-301 (1995).
23. Pitz, R. W., Brown, T. M., Nandula, S. P., Skaggs, P. A., DeBarber, P. A., Brown, M. S., and Segall, J., "Unseeded velocity measurement by ozone tagging velocimetry," *Opt. Lett.* **21**, pp. 755-757 (1996).
24. Ribarov, L. A., Wehrmeyer, J. A., Batliwala, F., Pitz, R. W., and DeBarber, P. A. "Ozone tagging velocimetry using narrowband excimer lasers," *AIAA Journal* **37**, 708-714 (1999).
25. Pitz, R. W., Wehrmeyer, J. A., Ribarov, L. A., Oguss, D. A., Batliwala, F., DeBarber, P. A., Deusch, S., and Dimotakis, P. E., "Unseeded molecular flow tagging in cold and hot flows using ozone and hydroxyl tagging velocimetry," *Meas. Sci. Tech.* **11**, 1259 (2000).
26. Boedeker, L. R., "Velocity measurement by H₂O photolysis and laser-induced fluorescence of OH," *Opt. Lett.* **14**, 473-475 (1989).
27. Davidson, D. F., Chang, A. Y., DiRosa, M. D., and Hanson, R. K., "Continuous Wave Laser Absorption Techniques for Gasdynamic Measurements in Supersonic Flows," *Appl. Opt.* **30**, 2598-2608 (1991).
28. Wehrmeyer, J. A., Ribarov, L. A., Oguss, and Pitz, R. W., "Flame flow tagging velocimetry with 193 nm H₂O photodissociation," *Appl. Opt.* **38**, 6912-6917 (1999).
29. Ribarov, L. A., Wehrmeyer, J. A., Pitz, R. W., and Yetter, R. A., "Hydroxyl tagging velocimetry (HTV) in experimental airflows," *App. Phys. B* **74**, pp. 175-183 (2002)

30. Ribarov, L. A., Wehrmeyer, J. A., Hu, S., and Pitz, R. W., "Multiline hydroxyl tagging velocimetry measurements in reacting and nonreacting experimental flows," *Experiments in Fluids*, **37**, 65-74 (2004).
31. Dam, N. J., Klein-Douwel, J. H., Sijtsma, N. M., and ter Meulen, J. J., "Nitric oxide flow tagging in unseeded air," *Optics Letters* **26**, 36-38 (2001).
32. Sijtsma, N. M., Dam, N. J., Klein-Douwel, J. H., and ter Meulen, J. J., "Air photolysis and recombination tracking: A new molecular tagging velocimetry scheme," *AIAA J.* **40**, 1061-1064 (2002).
33. van der Laan, W. P. N., Tolboon, R. A. L., Dam, N. J., and ter Meulen, J. J., "Molecular tagging velocimetry in the wake of an object in supersonic flow," *Exp. Fluid* **34**, pp. 531-533 (2003).
34. Miles, R. B. and Lempert, W. R., "Quantitative flow visualization in unseeded flows," *Ann. Rev. Flu. Mech.* **29**, pp. 285-326 (1997).
35. Noullez, A., Wallace, G., Lempert, W. R., Miles, R. B., and Frisch, U., "Transverse velocity increments in turbulent flow using the RELIEF technique," *J. Fluid Mech.* **339**, 287-307. (1997).
36. Ben-Yakar, A. and Hanson, R. K. "Cavity flame-holders for ignition and flame stabilization in scramjets: an overview," *J. Propul. Power* **17**, 869-877 (2001).
37. Gruber, M. R. and Nejad, A. S., "New supersonic combustion research facility," *J. Propul. Power* **11**, 1080-1083 (1995).
38. Gruber, M. R., Baurle, R. A., Mathur, T., and Hsu, K.-Y. "Fundamental studies of cavity-based flameholder concepts for supersonic combustors," *J. Propul. Power* **17**, 146-153. (2001)
39. Gruber, M. R., Donbar, J. M., Carter, C. D., and Hsu, K.-Y., "Mixing and combustion studies using cavity-based flameholders in a supersonic flow," *J. Propul. Power* **20**, 769-778 (2004).
40. Luque, J. and Crosley, D. R., LIFbase: Database and Spectral Simulation, SRI International Report MP99-009 (1999). <http://www.sri.com/cem/lifbase>
41. Gendrich, C. P. and Koochesfahani, M. M., "A spatial correlation technique for estimating velocity fields using molecular tagging velocimetry (MTV)," *Exp. in Fluids*, **22**, 67-77 (1996).
42. Cohn, R. K. and Koochesfahani, M. M., "The accuracy of remapping irregularly spaced velocity data onto a regular grid and the computation of vorticity," *Exp. in Fluids*, **29(1)**, S61-S69 (2000).
43. Pitz R. W. and Daily, J. W. "Combustion in a turbulent mixing layer formed at a rearward-facing step," *AIAA J.*, **21**, 1565-1570 (1983).

Table 1. Mach 2 Flow with a Wall Cavity

Test	Mach No.	Stagnation Conditions		Isentropic Conditions Mach = 2		Air Mass Flowrate	Water Mass Flowrate	Back Pressure Valve	Cavity Bottom Wall Pressure
		P_o	T_o	P	T				
		(kPa)	(K)	(kPa)	(K)	(kg/sec)	(g/sec)	%	(kPa)
A	2	170	520	22	290	1.4	25	0	35
B	2	170	520	22	290	1.4	25	64	70

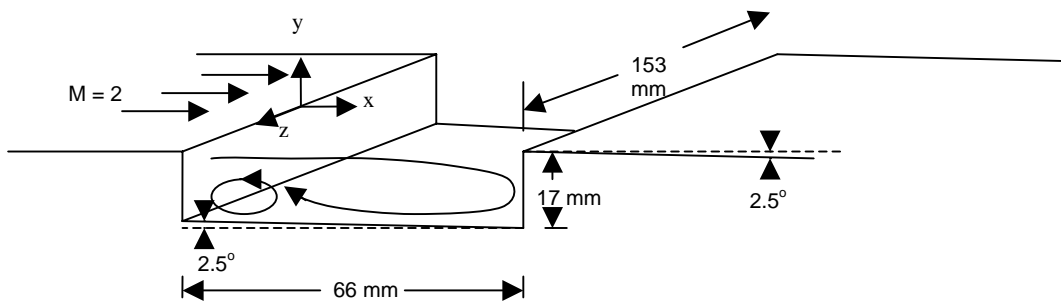


Fig. 1. Mach 2 Cavity Piloted Flow

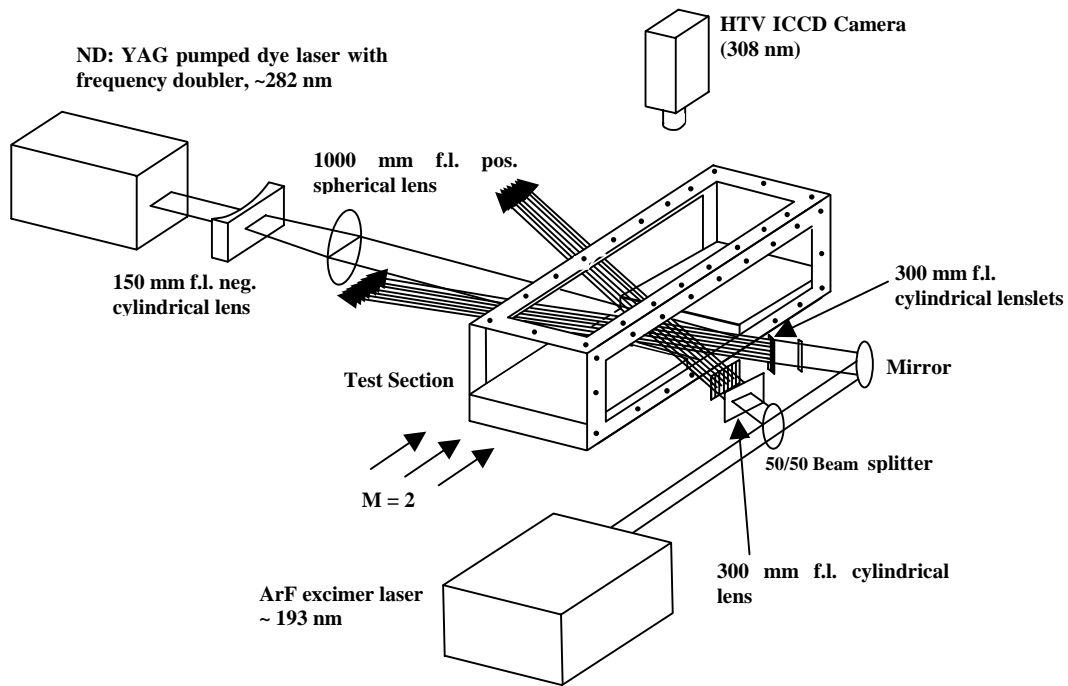


Fig. 2. Schematic of the HTV experimental system.

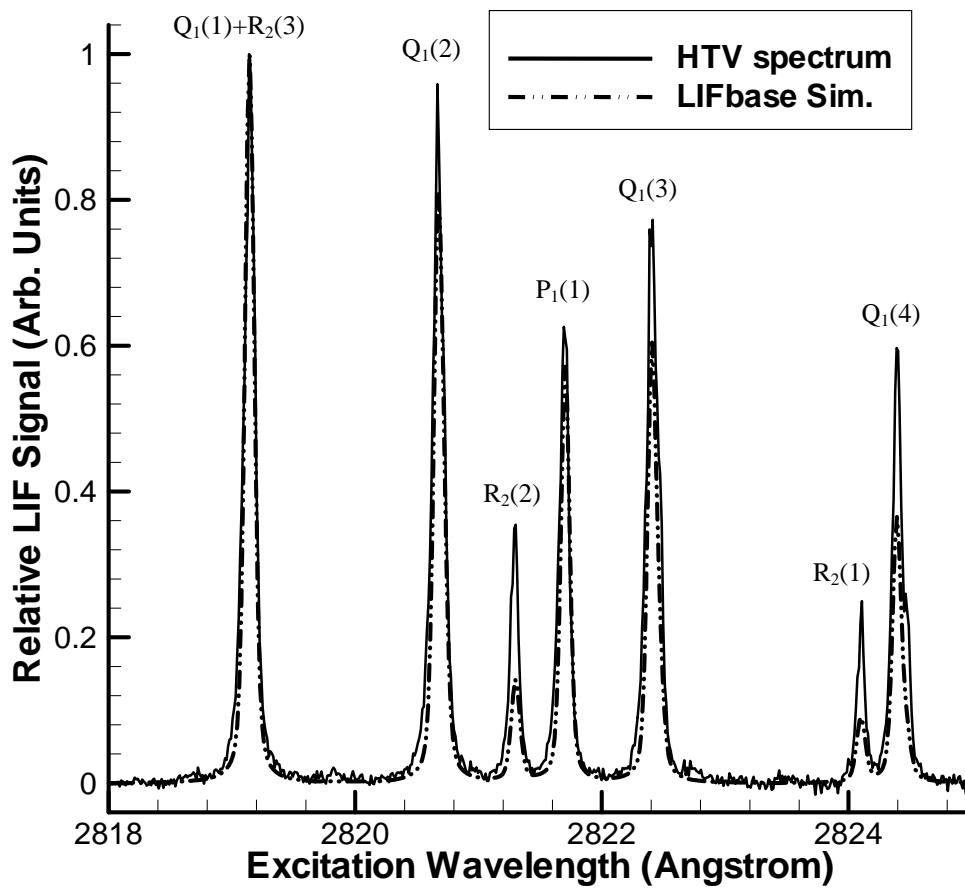


Fig. 3. Experimental and simulated excitation scans (relative to the $Q_1(1)$ signal) across OH A-X(1,0) transitions. Broadening of the simulated spectrum ($T=295$ K, LIFbase v. 2) was adjusted to match approximately the experimental spectrum; peak heights of the experimental and simulated $Q_1(1)+R_2(3)$ line were also matched. The experimental spectrum was derived from a sequence of 600 images, each image being the sum of 5 exposures of the grid at ~ 295 K and 745 Torr.

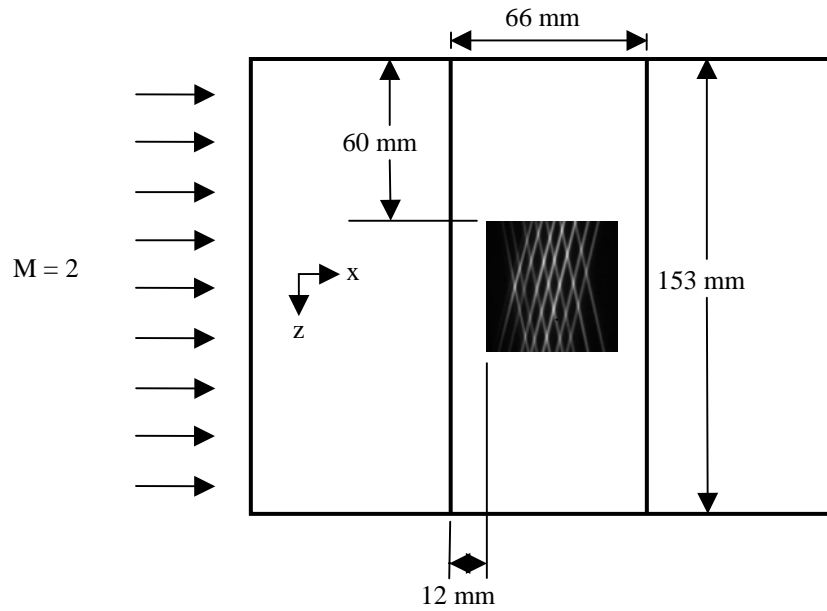


Fig. 4. Overhead schematic of the cavity, showing the position of the HTV images in regards to the cavity steps and test section walls.

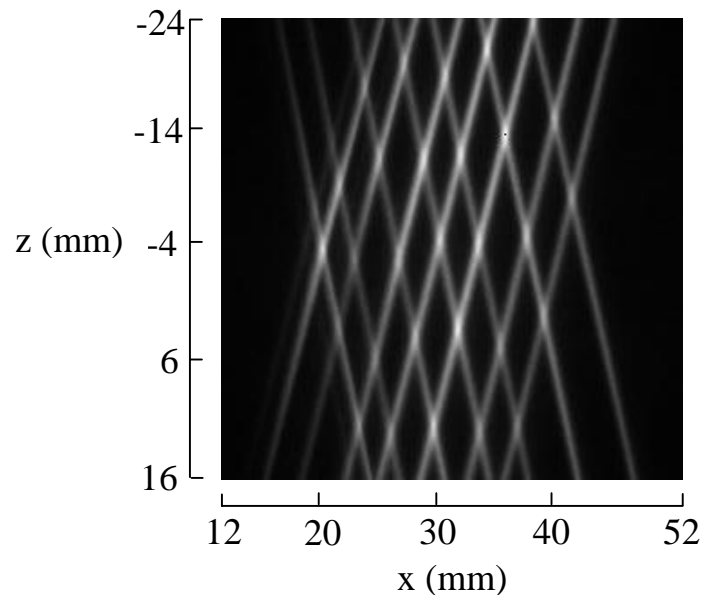


Fig. 5. Averaged un-delayed HTV image (at $y = 15.62$ mm, where $z=0$ is the centerline of the cavity and $x=0$ is at the front face of the cavity).

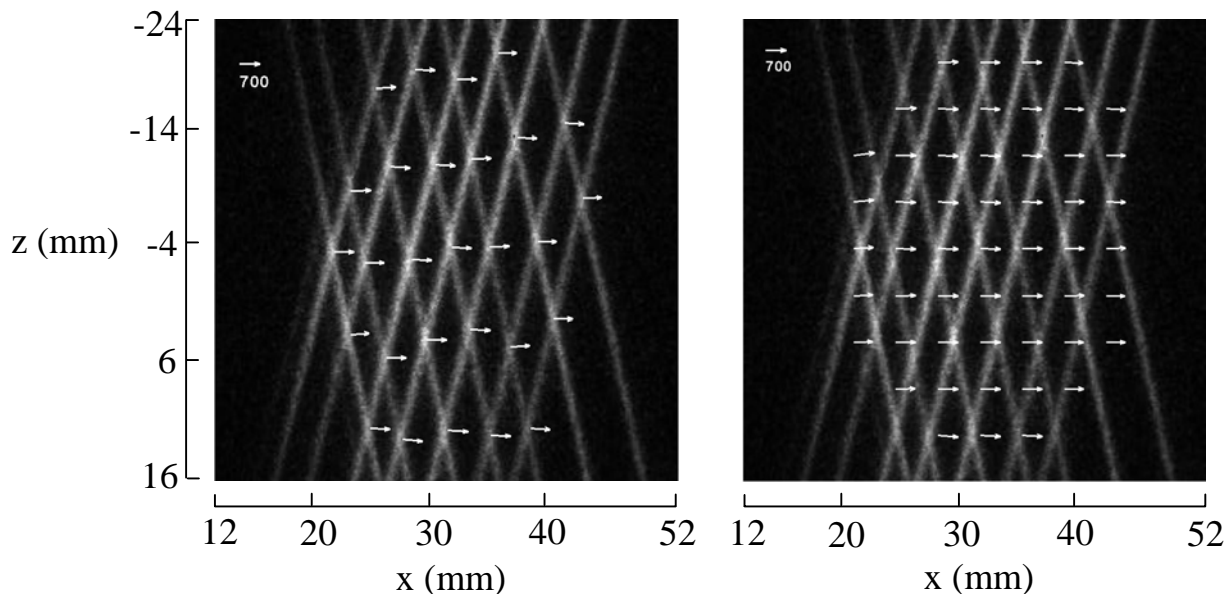


Fig. 6. Single-shot HTV images giving velocity images with an irregular (left) and regular grid (right) in a Mach 2 nonreacting scramjet cavity flow (at $y = 15.62$ mm, where $z=0$ is the centerline of the cavity and $x=0$ is at the front face of the cavity).

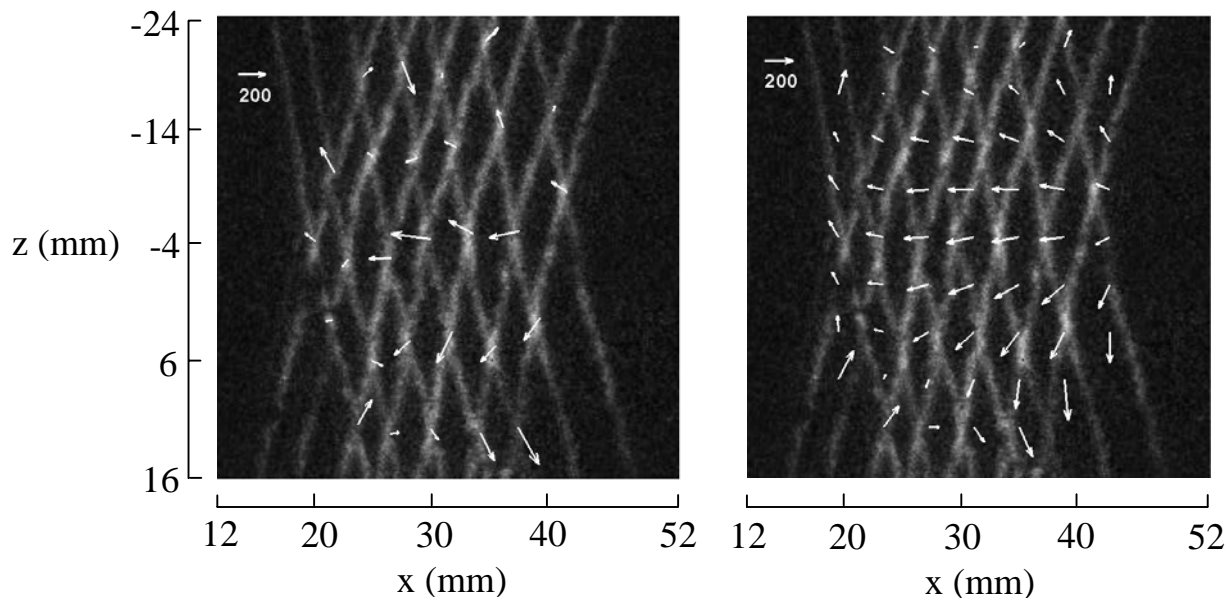


Fig. 7. Single-shot HTV images giving velocity images with an irregular (left) and regular (right) grid in a Mach 2 nonreacting scramjet cavity flow (at $y = -4.67$ mm, where $z=0$ is the centerline of the cavity and $x=0$ is at the front face of the cavity).

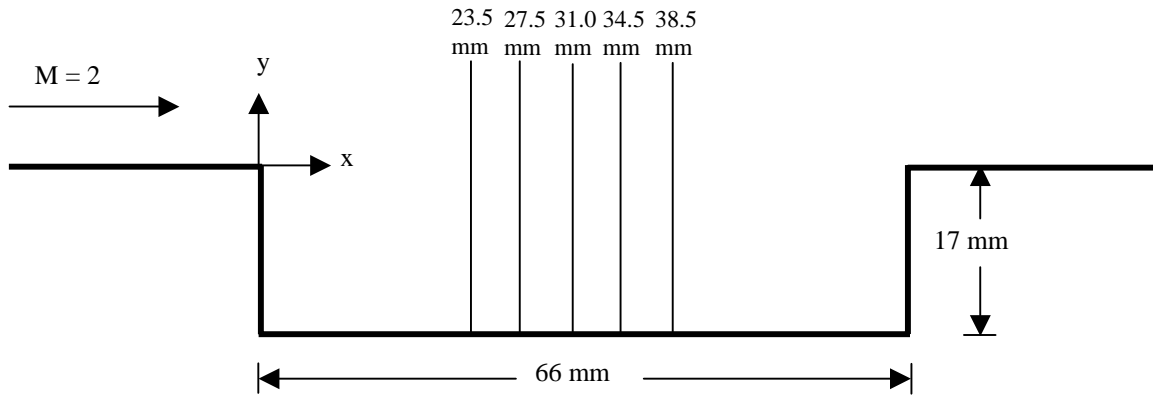


Fig. 8. Side-view schematic of the cavity, showing the profile locations along the x-axis.

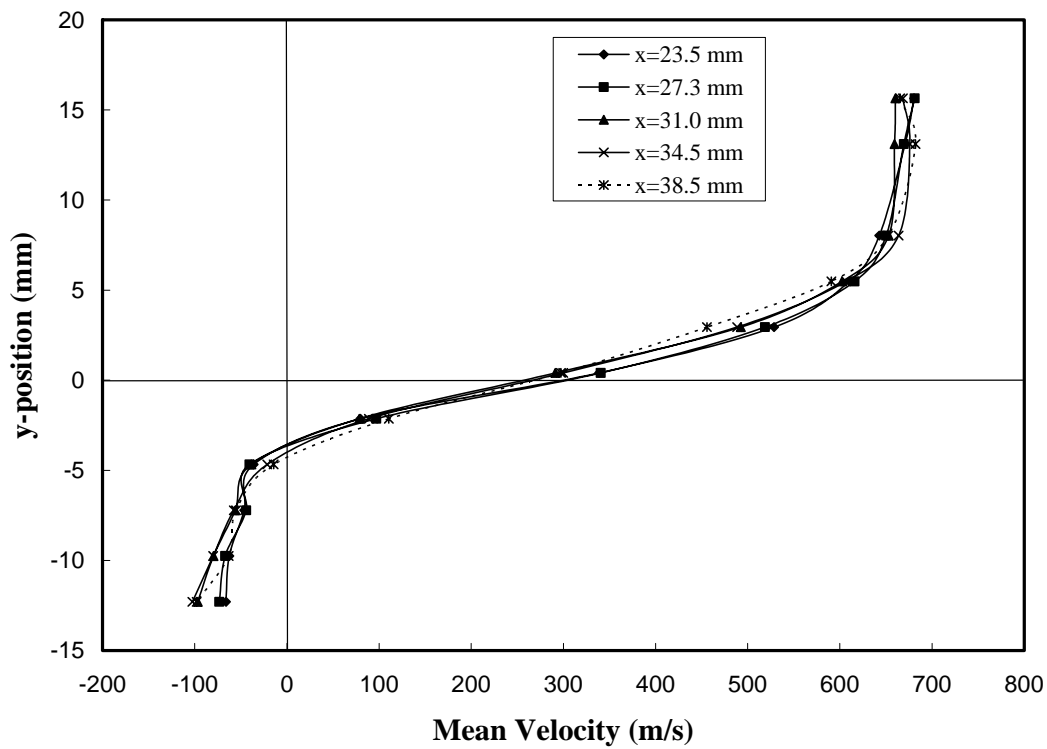


Fig. 9. Streamwise mean velocity profiles in the Mach 2 cavity flow showing shear layer between the freestream and the cavity at low backpressure conditions. (Near centerline, $z = -3.5$ mm where $z=0$ is the centerline of the cavity and $x=0$ is at the front face of the cavity)

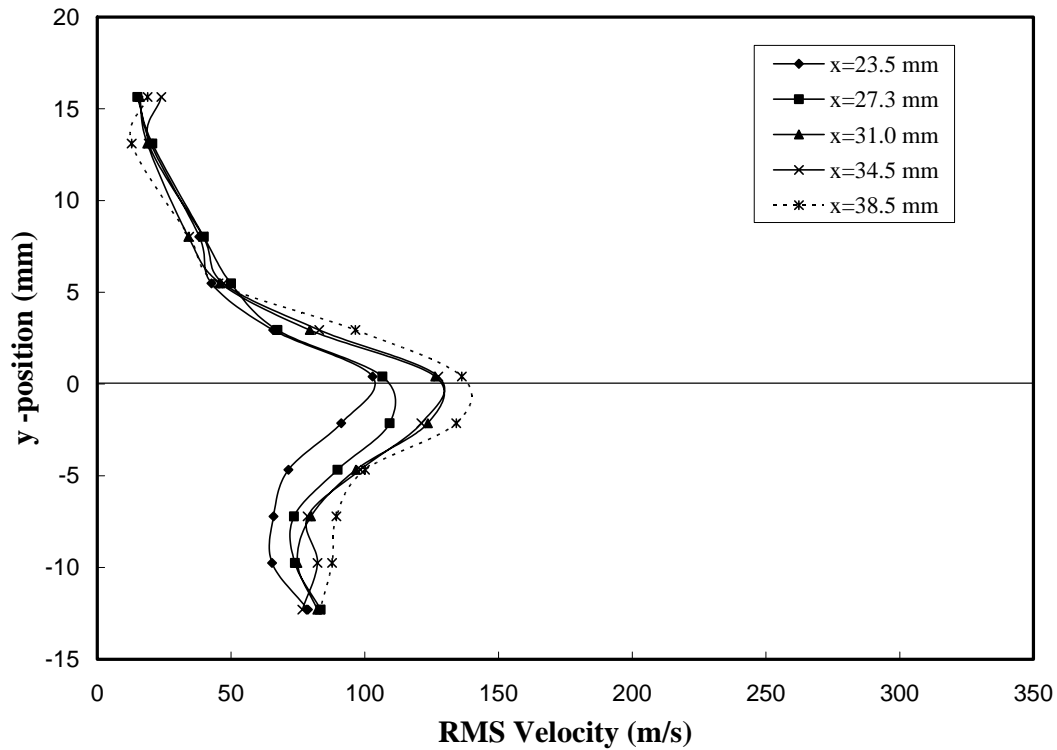


Fig. 10. Streamwise rms velocity profiles in the Mach 2 cavity flow showing shear layer between the freestream and the cavity at low backpressure conditions. (Near centerline, $z = -3.5$ mm where $z=0$ is the centerline of the cavity and $x=0$ is at the front face the cavity)

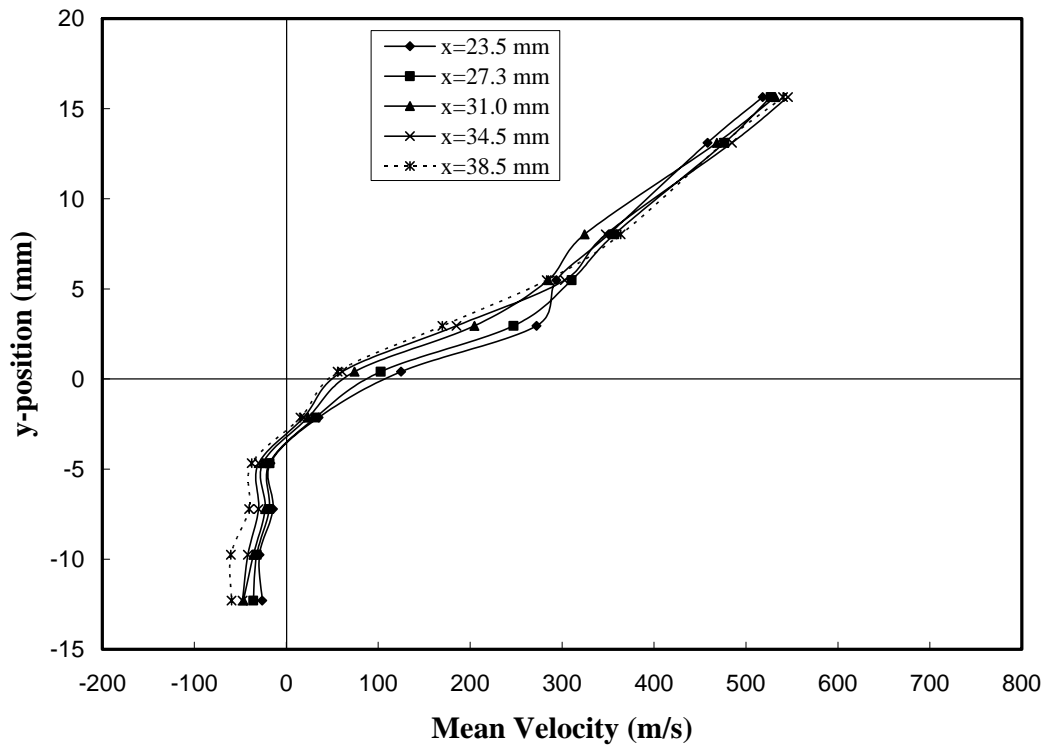


Fig. 11. Streamwise mean velocity profiles in the Mach 2 cavity flow showing shear layer between the freestream and the cavity at high backpressure conditions. ($z = -3.5$ mm where $z=0$ is the centerline of the cavity and $x=0$ is at the front face of the cavity)

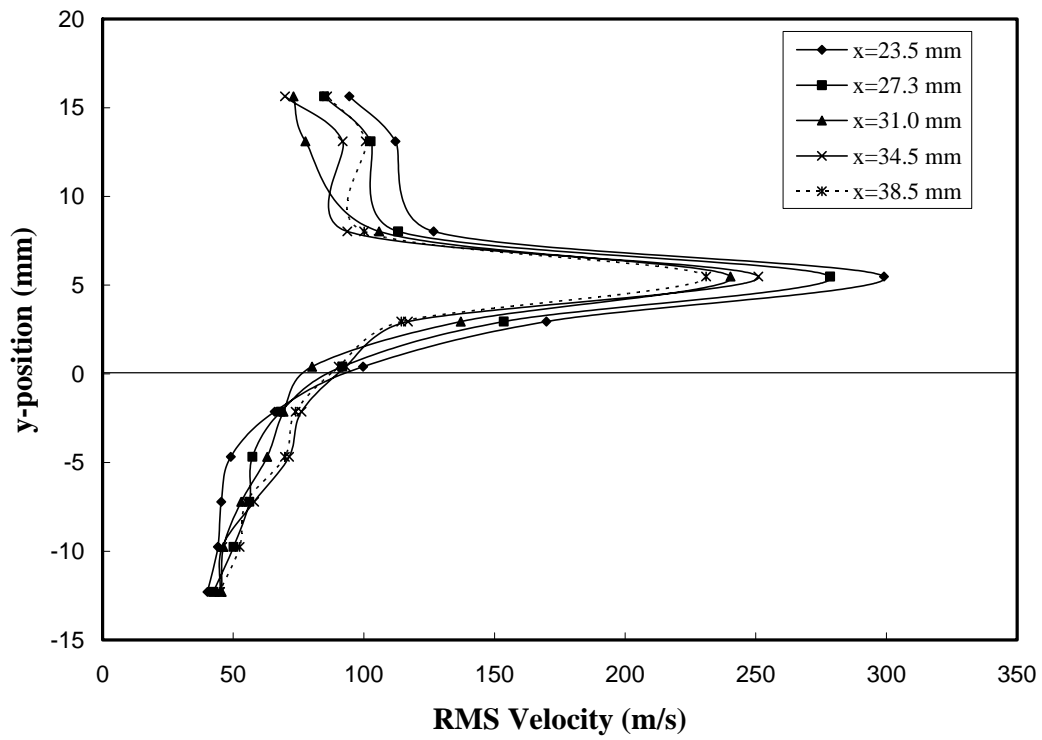


Fig. 12. Streamwise rms velocity profiles in the Mach 2 cavity flow showing shear layer between the freestream and the cavity under high backpressure conditions. ($z = -3.5$ mm where $z=0$ is the centerline of the cavity and $x=0$ is at the front face of the cavity)